First principle study of the adsorption of glyphosate on illite clay for water depollution.

.

ABSTRACT

The use of herbicides such as glyphosate in the agricultural sector enables agricultural intensification and thus satisfies the demand for agricultural products on the market. Glyphosate is widely used in agriculture as a herbicide for weeding fields. However, its use has a major drawback that calls into question its many advantages. After use, its toxic residues and metabolites end up in groundwater, which is an important source of drinking water for the population. Adsorption is the most suitable technique for recovering these toxic residues before the water is consumed. Based on Density Functional Theory, implemented in the VASP simulation code, we studied the ability of illite to adsorb glyphosate. The absorbent properties, the abundance of illite throughout the world, particularly in Benin, and the fact that it is free from toxic products were the criteria that guide us in the of illite clay for our work. Our work revealed that the process of adsorption of glyphosate on the illite surface is exothermic. This process does not present any risk of release of toxic by-products on five of the six studied sites. The illite clay can then be used to design water depollution filters to decrease medical as well as financial burden.

Keywords: Glyphosate; illite; DFT ; VASP ; adsorption

1. INTRODUCTION

Glyphosate is the active principle in herbicides used mainly to destroy weeds. [1],[2]. Thanks to the surfactants added to glyphosate[3], the molecule penetrates plants and blocks the biochemical processes that enable them to produce the aromatic amino acids that make up the building blocks of organic matter. As a result, plants are unable to grow and die. [4]. Every year, up to five billion kilograms of pesticides are reportedly applied worldwide, and it's expected to reach approximately 10 billion kilograms in 2050 [5],[6]. The use of glyphosate based herbicides would present many disadvantages and as a result, had been declared by the world organization of health, a dangerous compound for the environment and the health of human beings, mammals and birds. [7],[8] . Glyphosate is thought to have genotoxic effects on living organisms, a fact that places it at the origin of several pathological mechanisms, including cancer. Long-term exposure to glyphosate could also cause endocrine function disruption in humans [9],[10], attention-deficit/hyperactive disorder

(ADHD), colitis, diabetes, heart disease, inflammatory bowel disease, amyotrophic lateral syndrome, multiple sclerosis, obesity, depression, non-Hodgkin lymphoma and Alzheimer's disease, brain and breast cancer, birth defects, celiac disease and gluten intolerance [11]–[20].

Also, it has been evidenced that glyphosate and its derivatives can contaminate groundwater, surface waters (creeks, brooks, lakes, rivers and drains), marine sediments, seawater and rain [21]–[24]. Unfortunately, these contaminable water source constitute the main drinkable water sources of the population[25]. This contamination of water exposes human populations, aquatic fauna and flora to all these dangerous effects mentioned above [26]–[28]. It is therefore very important to find ways to reduce exposure to the glyphosate molecule, especially in least developed areas where access to drinking water is problematic, by removing glyphosate and its derivatives form contaminated water before their consumption.

To deal with this harmful environmental problem, many technics have been used, namely, chemical precipitation, microbial techniques, degradation, electrocoagulation, electrolysis; membrane extraction and adsorption [29],[30][31]–[33]. Among all these mentioned treatment techniques, adsorption is the most suitable for trapping this type of molecule because of its effectiveness. Indeed, the precipitation method for example, although having the possibility to allow the pollutant removal at a high rate, could release in the medium many other byproducts which management could be difficult [34].

Different materials are used as adsorbent in the adsorption of pollutants. Activated char materials are one the most used materials in this process [35],[36] given their large specific area [37], but have the drawback to be high costing, non-efficient in aqueous medium and non-easy to be regenerated [38]. Nanomaterial adsorbents, composite materials, soil and geominerals-like clays are also used for the removal of pollutant and particularly glyphosate from wastewater [39]–[42]. Among these materials, clays are of particular interest for adsorption. Indeed, after undergoing structural modifications, clays acquire a capacity similar

to that of activated carbons. This acquired capacity, added to their large specific surface areas, their swelling capacity, their cation exchange capacity and their availability in nature, make them more suitable for treating contaminated water. This could explain the important number of studies devoted to the use kaolinite and of pristine or modified montmorillonite, a smectite clay, to remove glyphosate from wastewaters [43]–[46]. In smectite clays,illite is also considered to treat wastewater [47]. To the best of our knowledge, no study has been devoted to glyphosate trapping with illite clay especially by a density functional theory (DFT) study. DFT method has this advantage to provide optimal orientations to how experiments should be conducted to avoid time wasting, uncertain high costing experiment protocols.

The aim of the present work was to perform atomistic simulation studies using DFT to explore the adsorption capacity of modified illite for glyphosate. To better suit experiment structure of illite clay used in this wok, we modified the basic illite primitive cell available in literature [48],[49]. So, illite modification led to a primitive cell containing 4 Al, 4 H, 2 K, 1 Mg, 24 O, 7 Si and 1 Na, where six potential adsorption sites called K, Na, Al, Si, O, and H were identified as described in Fig 1b. Adsorption energies of glyphosate on these six adsorption sites have been specifically calculated to elucidate adsorption mechanisms of glyphosate on illite.

2. COMPUTATIONAL DETAILS

2.1 MODELLING THE ADSORBENT AND ADSORBATE SYSTEMS

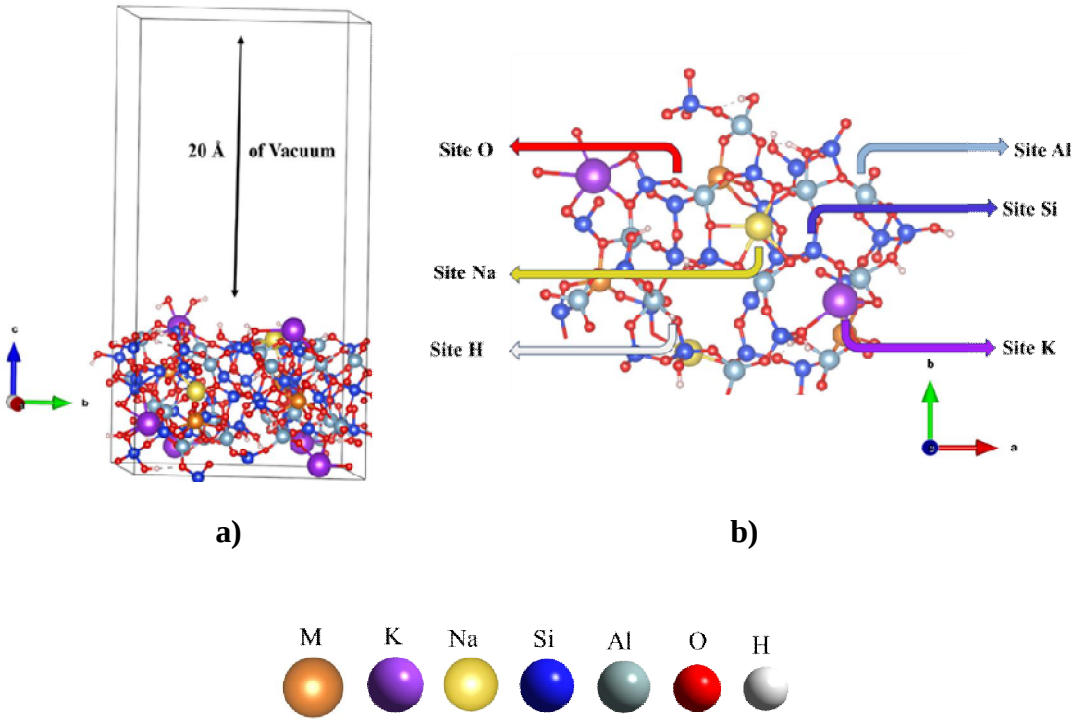

a) **b)**

Fig. 1. The cells used for DFT study, (a) Illite 3x2x1 supercell with 25 Å of vaccum along c, (b) adsorption sites viewed from the face (001).

The illite surface used for this work is a 3x2x1 supercell build from a modified and optimized primitive cell [50] , which has the structural parameters a = 5.20, b = 8.97, c = 8.97, α = 90.00°, β = 101.57°, and γ = 90.00°. The 3x2x1 was considered to both meet the Al/Si ratio experimentally found to be around 0.56 and the required space for the considered molecule to be adsorbed without stearic clash. The primitive cell was modified to insure the chemical composition found experimentally [48],[49]. So, the primitive cell contains 4 Al, 4 H, 2 K, 1 Mg, 24 O, 7 Si and 1 Na. The 3x2x1 build supercell was submitted to ab initio molecular dynamics (AIMD) simulation and the most stable geometry obtained was

optimized through static DFT calculation. To avoid any interaction between the adsorbed molecule and the periodic image of the slab, a vacuum of 20Å was systematically added along the c direction (**Fig. 1a**). Hence, the investigated surface corresponded (the (001) surface) to the main cleavage plan, that should allow the highest adsorption capability. We have identified six potential adsorption sites on the illite modelled surface hereafter called site-Al, sit-Si, site-K, site-Na, site-O and site-H (**Fig. 1b**).

2.2 CALCULATION METHODOLOGIES FOR EXPLOITING THE RESULTS

The calculations were carried out using periodic DFT theory as implemented in the theoretical calculation code Vienna Ab-Initio Simulation Package (VASP 5.4.1) [25]. Plan waves (PAW) were used to describe the valence electron interactions [51]. The core electrons were described using pseudopotentials. The convergence criterion for electron relaxation using the self-consistent solution of the Kohn-Sham equations is fixed at 10^{-6} eV. For ionic relaxations, calculations are allowed to converge as soon as the difference in force acting on each atom between two consecutive cycles is less than or equal to 0.02 eV/A. The Perdew-Burke-Ernzerhof (PBE) functional of the DFT, which resulted from the generalized gradient approximation (GGA), was used [52],[53]. For the optimizations of all the systems studied, Brillouin zone integration was performed with the Monkhorst-Pack algorithm using only the Γ point. This was indeed dictated by the large size of the systems studied.

The total density of states (TDOS) [54] were calculated on a finer grid (6×6×1). The plan wave cut-off energy was chosen to be 500 eV for all systems. To give a much more accurate description of the interactions occurring during adsorption processes, we took into account the dispersion forces in the calculations using Grimme's D2 method [53],[55]

The adsorption energy ΔE_{ads} of the glyphosate molecule on the illite surface was calculated according to the following formula:

$$\Delta E_{ads} = E_{Illite-glyphosate} - (E_{\text{glyphosate}} + E_{Illite}) \quad (1)$$

Where $E_{Illite-\text{glyphosate}}$ is the energy of the illite and the adsorbed chlorothalonil system, $E_{\text{glyphosate}}$ is the energy of the isolated glyphosate molecule and E_{Illite} is the energy of the illite surface.

The variation in electron density caused by the adsorption of the molecule onto the surface can help gaining more insight in the nature of interactions occurred during adsorption [56],[57]. It is calculated according to formula (2) below and visualized with the VESTA software [58].

$$\Delta\rho = \rho_{glyphosate\_Illite} - (\rho_{glyphosate} + \rho_{illite}) \quad (2)$$

With $\rho_{glyphosate\_Illite}$ being the electron density of the illite-glyphosate system after adsorption, $\rho_{glyphosate} and \rho_{illite}$ are respectively the electron densities of the chlorothalonil molecule and illite.

To assess the thermochemistry aspects of the performed adsorptions, we calculated the enthalpy and free enthalpy variation for the most stable configuration on each site. Given the big size of the studied systems,we allow only atoms of glyphosate molecule tomove during frequencies calculations while atoms of illite surface were frozen . Indeed, we assumed that all motions components in the surface will compensates before and after adsorption. Once the frequencies calculations were performed, we used vaspkit tool [59]to generate thermal corrections in the range of temperatures going from 300K to 600K with a step size of 50K. The enthalpy and free enthalpy variations (ΔH_{ads}, ΔG_{ads}) are calculated as follow:

$$\Delta H_{ads} = \Delta E_{ads} + \Delta ZPE \quad (3)$$

$$\Delta G_{ads} = \Delta E_{ads} + \Delta ZPE - T\Delta S_{ads} \quad (4)$$

ΔZPE is the variation of zero-point energy of the adsorption process and ΔS the entropy variation.

3. RESULTS AND DISCUSSION

Figure 2 below shows the structure of the glyphosate molecule.

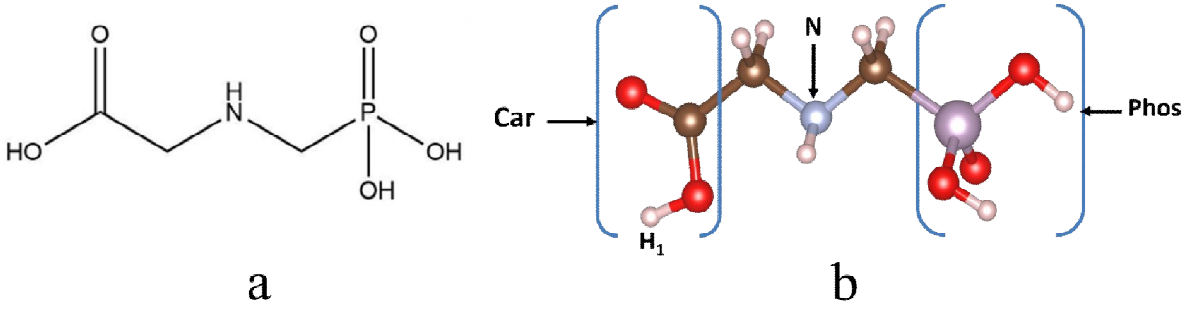

Fig. 2. Structure of glyphosate: a) 2D representation with numbering of the atoms through which glyphosate adsorbs to illite, b) 3D representation

Many adsorption configurations have been tested on each site of the illite surface. Indeed, three configurations have been obtained by directing toward the considered site on the illite surface each group (Car, N, Phos) highlighted on **Fig. 2b**when stearic effect do not prevent it. The fourth configuration was obtained by setting the glyphosate molecule in a plan parallel to the surface (Flat). The tested configurations will be hereafter referred to as follow: Car-X, N-X, Phos-X, Flat-X where X represents the site.

3.1. ADSORPTION ENERGIES

3.1.1 POTASSIUMSITE

The geometries and the adsorption energy of glyphosate molecule on the site K in all the configurations after adsorption are presented on **Fig. 3** below.

The analysis of adsorption energies reveals that the glyphosate molecule adsorbs more strongly in the N-K configuration. This is followed by the Flat-K, Phos-K and finally Car-K configurations. The adsorption energy of glyphosate in its N-K configuration is -238.83 kJ/mol with a dispersion energy of -56.25 kJ/mol corresponding to 23.25% of the total energy.

On this site, adsorption is dominated by chemical interactions due to the low contribution of van der Waals interactions. The adsorption of glyphosate on the Site-K of the illite surface

can therefore be done according to all tested configurations. The Car-K configuration, although possible because of the negative adsorption energy, is the least favorable.

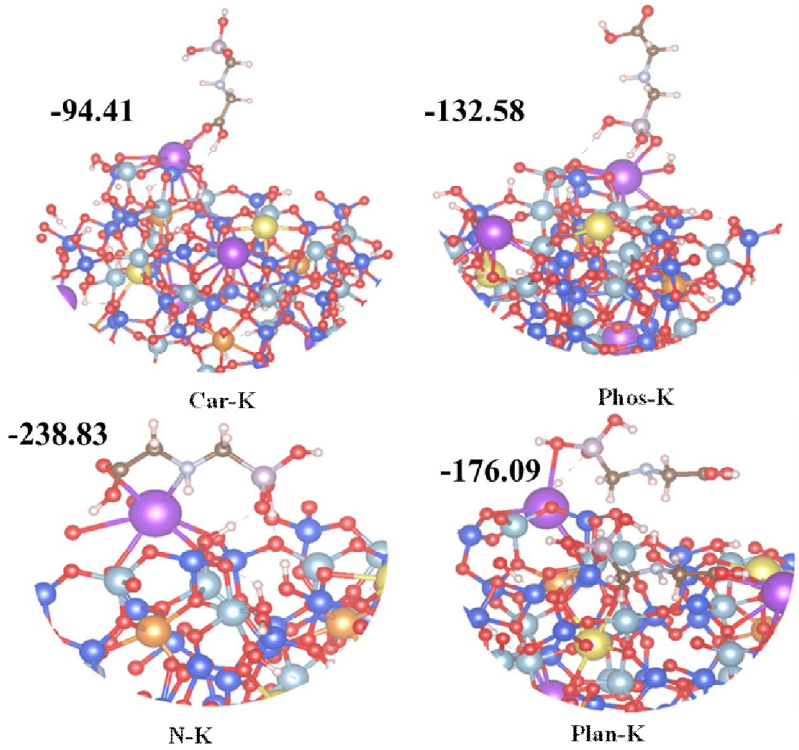

Fig. 3. Final geometries of glyphosate adsorption on K site of the illite surface and adsorption energies in kJ/mol

The final geometry of glyphosate adsorption on illite in this N-K configuration showed the formation of two bonds between a potassium atom on the illite surface and a nitrogen atom and an oxygen atom of the glyphosate. In addition, two hydrogen bonds were formed between oxygen and hydrogen atoms on the illite surface and on the glyphosate. All these bonds formed during the adsorption of glyphosate on the Site-K better explain the high adsorption energy obtained as well as the contribution in dispersion energy.

3.1.2 SODIUMSITE

As in the previous case, glyphosate was adsorbed on the sodium site (Site-Na) of illite. The adsorption energies and geometries of the configurations after adsorption are shown in **Fig. 4**.

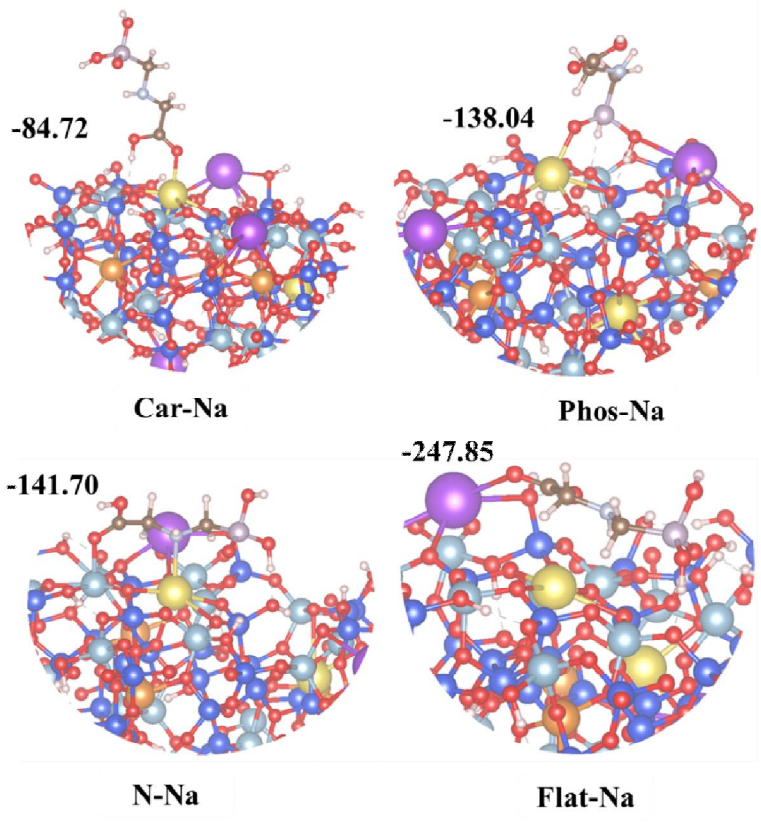

Fig. 4. Final geometries of glyphosate adsorption on sodium site of the illite surface and adsorption energies in kJ/mol

On the Na site, the glyphosate molecule can adsorb in several configurations. Indeed, for all the configurations modelled, the adsorption energies are negative. The Flat-Na configuration is the one in which the interaction of the glyphosate molecule with the illite surface is the strongest, with an adsorption energy of -247.85 kJ/mol including a dispersion energy of -78.93 kJ/mol (31.85%). Adsorption in this configuration is dominated by chemical

interactions with a prevalence rate around 68%. The Car-Na configuration is the least favored, as in the case of the K site.

In the final geometry of Flat-Na configuration, the adsorption of glyphosate on the sodium site of the illite was achieved by the formation of a bond between an oxygen atom of the glyphosate and a potassium atom on the illite surface. In addition, four hydrogen bonds were formed between oxygen and hydrogen atoms on the surface and the glyphosate molecule. These different bonds formed justify that the adsorption of the molecule is stronger in this configuration on this site.

3.1.3 SILICIUM SITE

The glyphosate molecule was also adsorbed on the silicon site (Site-Si) of the illite. The adsorption energies obtained (**Fig. 5)** are all negative and indicate that the glyphosate molecule can adsorb onto the Si site of the illite surface modelled in many configurations. The Flat-Si configuration is the most stable with an adsorption energy of -213.42 kJ/mol including a dispersion of -64.63 kJ/mol (30.28% of the total adsorption energy). Chemical interactions play the major role in the adsorption process. The H-Car-Si configuration is the least stable, as in the case of the two previous sites.

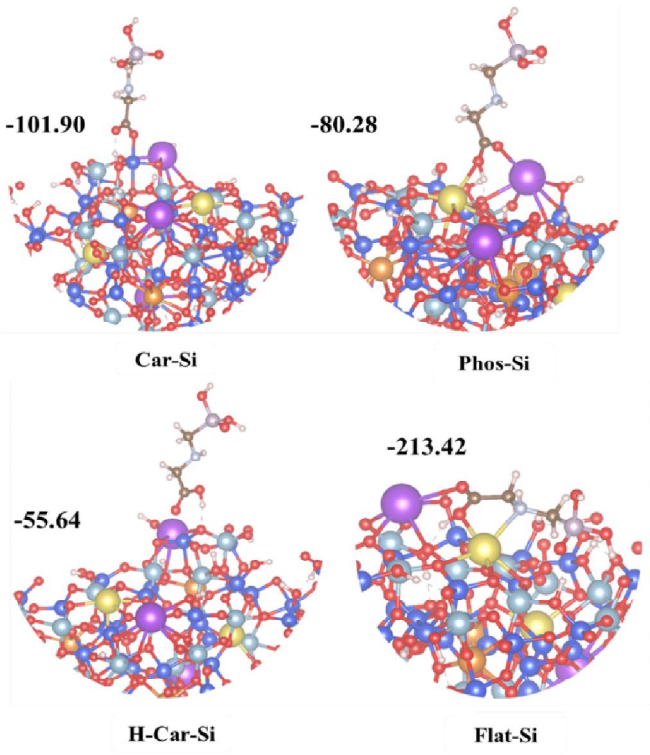

Fig.5. Final geometries of glyphosate adsorption on Si site of the illite surface and adsorption energies in kJ/mol

The adsorption of glyphosate in the most stable configuration (Flat-Si) occurred with the formation of a bond between a potassium atom on the surface and an oxygen atom of the glyphosate, and two bonds between a sodium atom on the surface and an oxygen atom and the nitrogen atom of the glyphosate. The formation of these different bonds explains the high adsorption energy value obtained, indicating the strong adsorption of glyphosate on this site in this configuration. In addition, this final geometry reveals the formation of three hydrogen bonds.

3.1.4 ALUMINUMSITE

Adsorption of glyphosate molecule on the illite surface has also been simulated on the aluminum site of the illite surface. The obtained adsorption energies and the geometries of the configurations after adsorption are presented on **Fig. 6.**

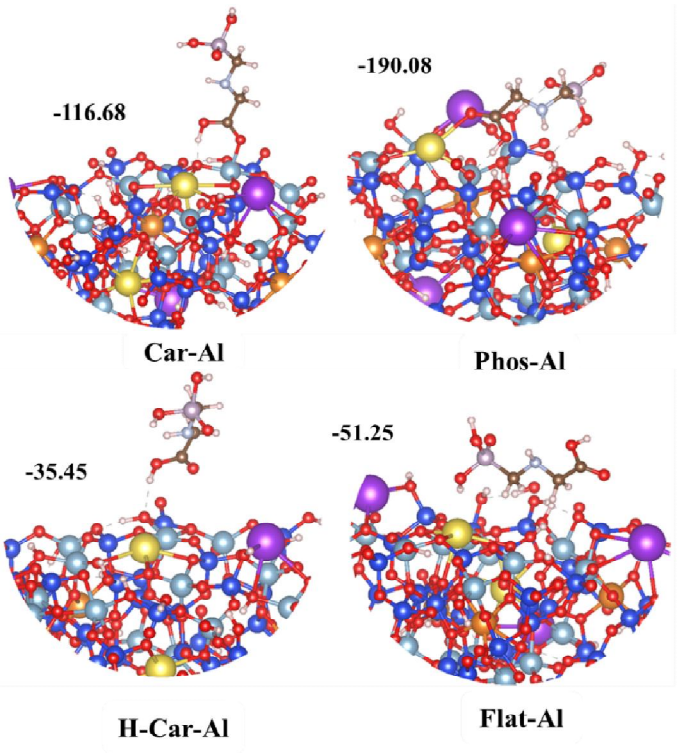

222

223 **Fig. 6. Final geometries of glyphosate adsorption on Al site of the illite surface and**
224 **adsorption energies in kJ/mol**

225 The information in Figure 6 reveals that the glyphosate adsorption process on the aluminum
226 site is exothermic since the adsorption energies for all the configurations are negative. We
227 note a strong adsorption of glyphosate on the Aluminum site of illite in the vertical
228 configuration (O-Phos-Al) with an adsorption energy of -190.08 kJ/mol. The dispersion
229 energy during this adsorption process is -61.36 kJ/mol, representing 32.28% of the total
230 adsorption energy. In this most stable configuration, adsorption occurred through the
231 formation of a bond between a sodium atom on the surface and an oxygen atom on the
232 glyphosate molecule. Three hydrogen bonds were also formed between oxygen and
233 hydrogen atoms. All the bonds formed justify the relative stability of this configuration
234 compared with the others.

235

3.1.5 OXYGENSITE

The glyphosate molecule was adsorbed on the oxygen site (Site-O) of the illite and the adsorption energies obtained are shown in **Fig. 7**bellow.

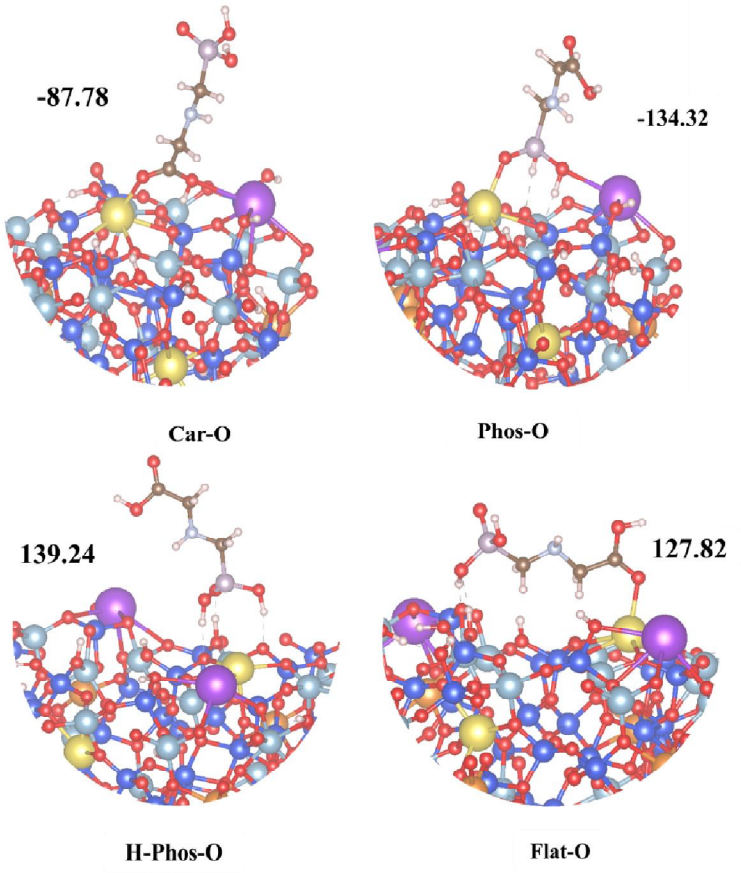

Fig. 7. Final geometries of glyphosate adsorption on O site of the illite surface and adsorption energies in kJ/mol

Analysis of **Fig. 7** reveals that strong adsorption of glyphosate on the oxygen site of illite is observed for all the configurations. Apart from the Car-O configuration which has a relatively low adsorption energy, the other configurations have almost equal but high adsorption energies. This indicates that glyphosate can adsorb to the O site of aluminum in several configurations. However, the H-O configuration is the one with the highest adsorption energy

in absolute values. The adsorption energy of glyphosate on the Oxygen site of illite in the most stable vertical H-O configuration is -139.24 kJ/mol with a low dispersion energy (24.10 kJ/mol). This dispersion energy is evaluated at 17.31% of the total adsorption energy. The Adsorption in this configuration is thought to be largely guided by chemical interactions.

The final geometry of glyphosate adsorption on the illite oxygen site in the H-O configuration shows the formation of three hydrogen bonds, one between a glyphosate oxygen atom and a hydrogen atom on the surface, and two others between two glyphosate hydrogen atoms and a nitrogen atom and an oxygen atom on the surface.

3.1.6. HYDROGENSITE

The adsorption potential of illite via the hydrogen site (Site-H) with respect to glyphosate was investigated using various configurations. The **Fig.9.** below provides information on the adsorption energies obtained and also on the geometries of configuration after adsorption.

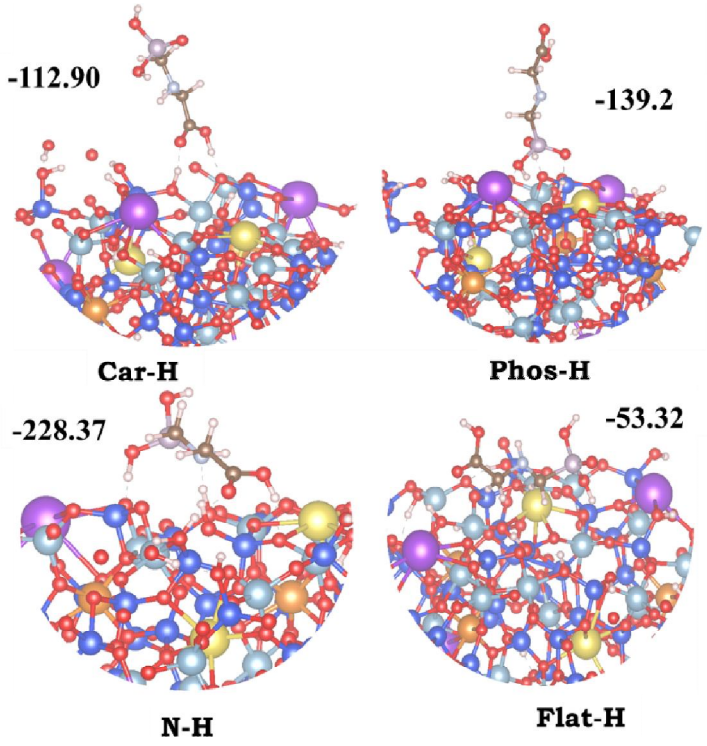

Fig.9. Final geometries of glyphosate adsorption on H site of the illite surface and adsorption energies in kJ/mol.

Analysis of the adsorption energies of glyphosate on the H site of illite (Figure 9) shows that the process is also exothermic as in the other cases. On this site, the configuration where the nitrogen atom of the glyphosate molecule is oriented towards the hydrogen atoms on the surface is the most stable. This was followed in that order by the Phos-H, Carb-H and finally Flat-H configurations. The adsorption energy in the N-H configuration is -228.37 kJ/mol with a dispersion energy of -74.98 kJ/mol. This dispersion energy represents 32.83% of the total adsorption energy. The adsorption has a prevalence of chemical interactions.

In the final geometry of glyphosate adsorption on the illite Hydrogen site in the N-H configuration, four hydrogen bonds were formed. Two are established between two oxygen atoms of glyphosate and two hydrogen atoms of the surface, and the other two, between two oxygen atoms of the surface and two hydrogen atoms of glyphosate.

3.1.7 COMPARATIVE STUDY OF ADSORPTION SITES.

From the previous analyses, we have identified, by site, the configurations in which glyphosate is strongly adsorbed onto illite surface. The diagram in **Fig. 10.** below shows the adsorption energies of glyphosate on illite according to the most stable configurations per site.

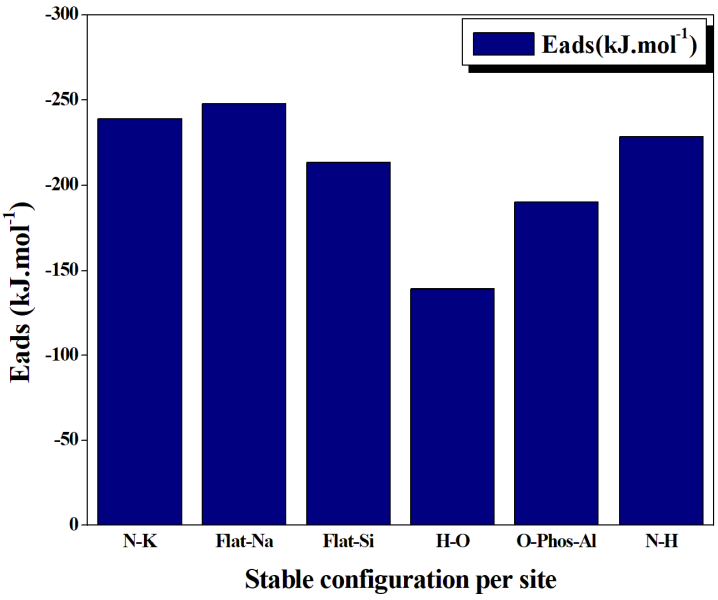

Fig. 10.Most stable Configurations per site during the adsorption of glyphosate molecule on illite surface.

Analysis of this histogram reveals that glyphosate adsorption is favorable on the six different sites explored. Adsorption was very strong on the sodium site, followed by the potassium, hydrogen, silicon, aluminum and oxygen sites. On the Sodium and Silicon sites, adsorption took place in a flat configuration, but in vertical arrangements on the other sites. Furthermore, given the low dispersion rate in the total adsorption energies, we can conclude that all the adsorptions were guided by chemical interactions.

3.2 Thermochemistry of adsorptions

To state out the exothermicity or endothermicity of the performed adsorptions, we calculated the enthalpy and the free enthalpy variations using relations (3) and (4) of subsection 2.2. The obtained values for both data are plotted on graphs of **fig. 11.** below.

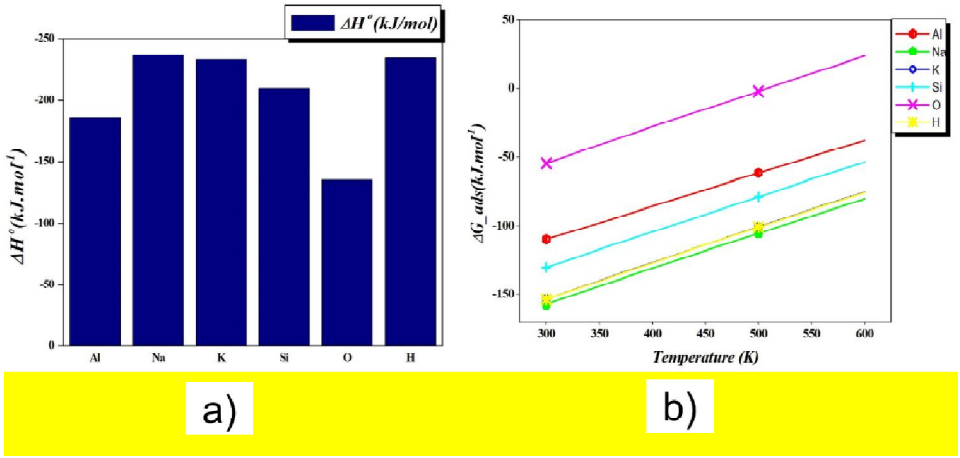

Fig. 11. Thermodynamic of the most stable configuration: a)variation of enthalpy, b) variation of free enthalpyalongwithtemperature

Analyzing the graph a) of fig. 11. It comes out that adsorption process is exothermic on all the sites, this because, all the ΔH_{ads}calculated are negative. Considering ΔH_{ads}, the oxygen site is also the less favored for the adsorption of glyphosate molecule on the considered illitesurface.Also, all calculated ΔG_{ads} are negative meaning that adsorptions are all spontaneous. Oxygen site is also the less favored when taking into account ΔG_{ads} analysis. The desorption temperature, corresponding to the temperature from whichΔG_{ads} will become positive, apart from the oxygen site, will be very high given thatΔG_{ads} is negative for all remaining sites even at temperatures beyond 600K.This could mean that desorption rate will be very low.

3.3 ADSORPTION MECHANISM

3.2.1 ASSESSMENT OF THE RISK OF FORMATION OF TOXIC BY-PRODUCTS

We calculated the length variation ofbonds containing atoms directly involved in the adsorption of glyphosate onto illite surface in order to assess the risk ofthe formation after adsorption of by-products that could be toxic. The histogram presented in **Fig. 12**below

311 shows the variation in the interatomic distances of the bonds involved after the adsorption of
312 glyphosate on illite for the most stable configurations per site.

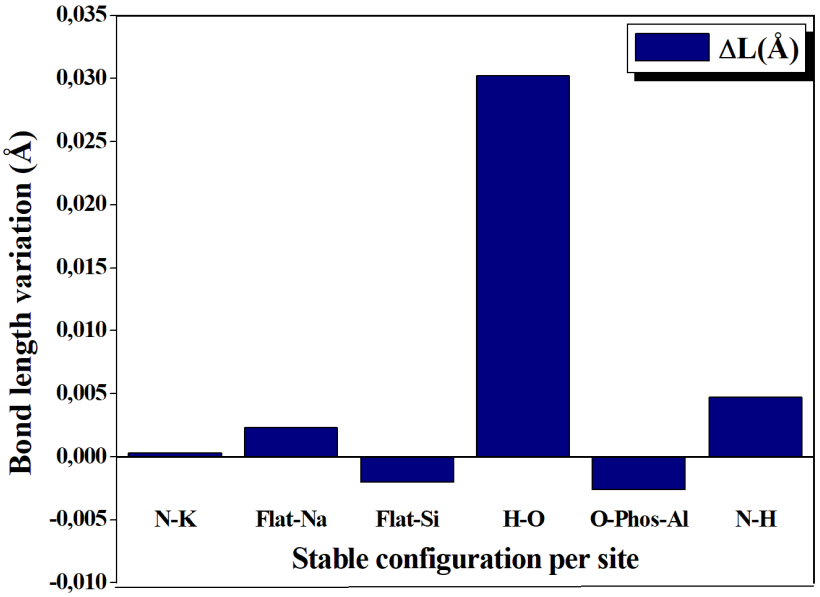

313

314 **Fig. 12. Variation in the bond lengths directly involved in the adsorption of glyphosate**
315 **on illite surface for the most stable configurations**.

316 The analysis of the graph in **Fig. 12** shows slight stretching of the bonds involved in
317 adsorption for the stable configurations of the K, Na and H sites. The elongation of the bond
318 at the Hydrogen site is 0.005 Å, followed by those at the Sodium and Potassium sites. For
319 the Silicon and Aluminum sites, we observed a shortening of the bonds involved. For the
320 Oxygen site, we note a significant stretching of the bond involved. The variation in
321 interatomic distance calculated is 0.030Å greater than the threshold value (0.02Å) for the
322 plausible formation of toxic by-products.

323 We therefore conclude that the glyphosate adsorption process on illite at the oxygen site
324 could present a risk of releasing toxic by-products. On the other sites, however, adsorption is
325 favorable and there is no risk of toxic by-products being formed. Oxygen site being the least

stable among the most stable configurations, one can conclude that there is no risk of by-product formation, a fact that can enhance the material recuperation for it reuse.

3.2.2 ISO-SURFACE ANALYSIS

To better elucidate the interactions that occurred during the adsorption of the glyphosate molecule onto illite, we plotted the iso-surfaces variation for two configurations identified as among the most stable on the sites Si and O as shown in **Fig. 13.** below.

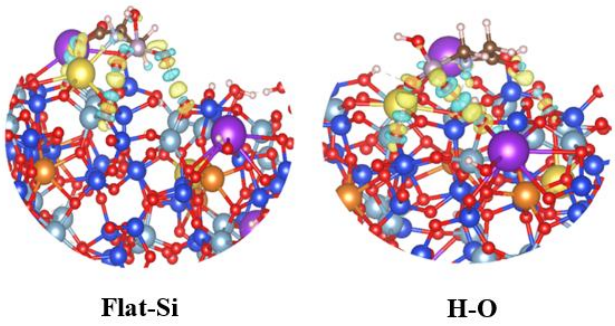

Fig. 13. **The electron density changes iso-surface for the stable configuration on Si and O Sites. The yellow and blue represented iso-surfaces indicate variations of +0.0015 and -0.0015 electron/Å^3, respectively**.

Analysis of **Fig. 13.**shows that in the stable configuration of the Si site, hydrogen bonds and electrostatic interactions between the nitrogen atom and the cations on the surface were formed, unlike in the H-O configuration where hydrogen bonds were mainly present. This justifies the fact that the adsorption energy at the Si site is higher and the configuration is more stable.The fact that electrostatic interactions and hydrogen bonds are the main parts of forces ruling the simulated adsorptions is line with conclusion of the work of Wang and coauthors[60].They conducted both experimental and theoretical study of the adsorption of glyphosate on montmorillonite clays and found that glyphosate adsorbed onto the montmorillonite clay, which is a smectite as illite, through electrostatic interactions and hydrogen bonding.

3.2.3 TOTAL DENSITY OF STATES (TDOS) ANALYSIS

In order to complete the understanding of the interactions between the illite surface and glyphosate molecule, the total densities of states are calculated for two of the most stable configurations (Flat-Si and H-O) per site after adsorption of glyphosate onto illite (**Fig. 14)**.

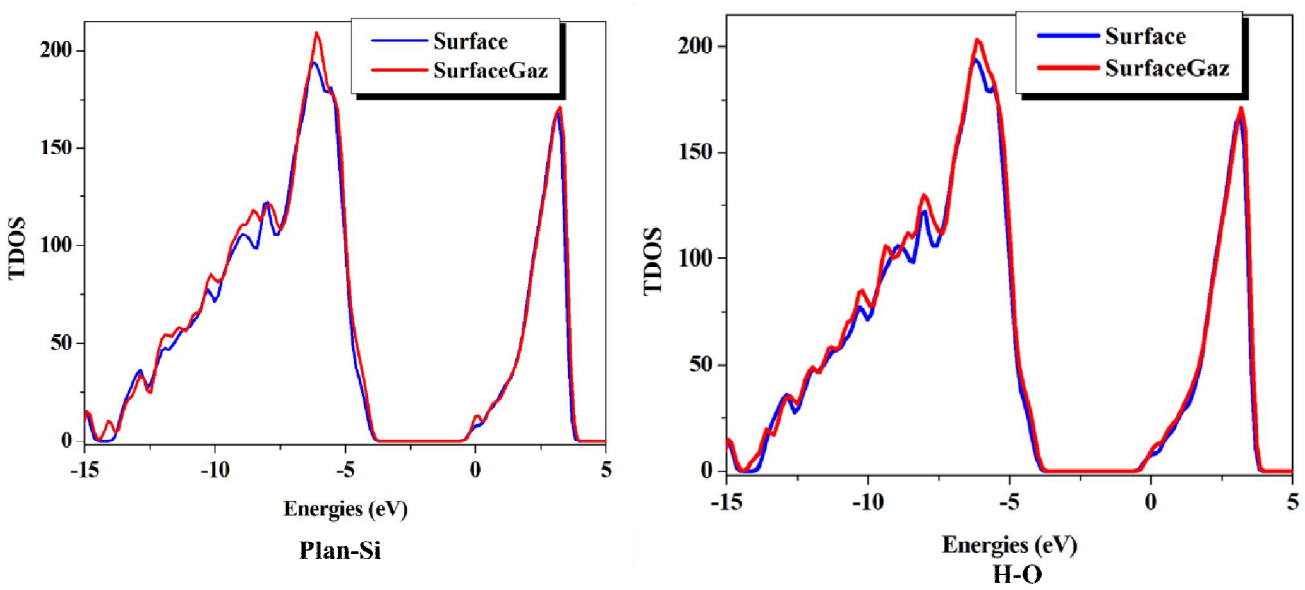

Fig. 13.Total densities of states of chlorothalonil adsorption on illite for the most stable configurations for site Si and O.

The analysis of the total density of state graphs for the stable configurations on the Si and O sites shows that the peaks became more intense after adsorption. In addition, new peaks appeared on the flat-Si configuration, which is more stable than the H-O configuration. These changes attest the great electronic reorganization that occurred during the adsorption processes. It is also very important to note that the electronic changes at the surface are greater for the flat-Si configuration than for the H-O configuration.

4. CONCLUSION

We conducted the DFT study of the adsorption of glyphosate on illite. The results of this work brought out the capability of illite clay modelled in this work to trap glyphosate molecule. We firstly assessed the adsorption energies of glyphosate molecule on illite and secondly, elucidated the adsorption mechanism at the surface through the nature of the interactions produced during adsorption. It globally comes out from this study that:

- the adsorption of glyphosate on the illite surface is exothermic,

- the process of adsorption of glyphosate on illite does not present any risk of release of toxic by-products on five of the six studied sites,

- The adsorption process in mainly under chemical control in almost all the cases

All this findings elect illite clay as a performant material to design filters for the depollution of waters contaminated with glyphosate and its derivatives. We planned to extend this work to other materials and also to consider conducting the study in aqueous area.

COMPETING INTERESTS

Authors have declared that no competing interests exist

AUTHORS' CONTRIBUTIONS

Wilfried G. KANHOUNNON: wrote the protocol, supervised the theoretical calculations, write parts of the manuscript

Orou Abdal Afiz Bana N'DOURO: Performed theoretical calculations and wrote some parts of the manuscript

Ezékiel LOKONON: Performed theoretical calculations and wrote some parts of the manuscript

Guy A. S. ATOHOUN: Supervised all the steps of the whole work

Gaston A. KPOTIN: Designed the study and supervised the manuscript writing

All authors read and approved the final manuscript

CONSENT (WHEREEVER APPLICABLE)

Not applicable

ETHICAL APPROVAL (WHEREEVER APPLICABLE)

Not applicable

REFERENCES

[1] Castillo-Villalón P, Ramírez J, Cuevas R, Contreras R, Luna R, Vaca H, Murrieta F. TPR-S analysis of the catalytic behavior of Ru/Al2O3 catalysts in industrial conditions 2005;Catal. Today 107–108:913–9. https://doi.org/10.1016/j.cattod.2005.07.154.

[2] Woodburn AT. Glyphosate: production, pricing and use worldwide. *Pest Manag Sci* 2000;56(4):309–12. https://doi.org/10.1002/(SICI)1526-4998(200004)56:4<309::AID-PS143>3.0.CO;2-C

[3] Tsui MTK, Chu LM. Aquatic toxicity of glyphosate-based formulations: comparison between different organisms and the effects of environmental factors. *Chemosphere* 2003;52(7):1189–97. https://doi.org/10.1016/S0045-6535(03)00306-0

[4] Sutton RF. Glyphosate Herbicide: An Assessment of Forestry Potential. *For Chron* 1978;54(1):24–8. https://doi.org/10.5558/tfc54024-1

[5] Özkara A, Akyil D, Konuk M. Pesticides, Environmental Pollution, and Health. In: Larramendy M, Soloneski S, eds. Environ. Health Risk - Hazard. Factors Living Species. InTech; 2016; https://doi.org/10.5772/63094

[6] Popp J, Pető K, Nagy J. Pesticide productivity and food security. A review. *Agron Sustain Dev* 2013;33(1):243–55. https://doi.org/10.1007/s13593-012-0105-x

[7] Valle AL, Mello FCC, Alves-Balvedi RP, Rodrigues LP, Goulart LR. Glyphosate detection: methods, needs and challenges. *Environ Chem Lett* 2019;17(1):291–317. https://doi.org/10.1007/s10311-018-0789-5

[8] Williams GM, Kroes R, Munro IC. Safety Evaluation and Risk Assessment of the Herbicide Roundup and Its Active Ingredient, Glyphosate, for Humans. *Regul Toxicol Pharmacol* 2000;31(2):117–65. https://doi.org/10.1006/rtph.1999.1371

[9] Gasnier C, Dumont C, Benachour N, Clair E, Chagnon M-C, Séralini G-E. Glyphosate-based herbicides are toxic and endocrine disruptors in human cell lines. *Toxicology* 2009;262(3):184–91. https://doi.org/10.1016/j.tox.2009.06.006

[10] Chalubinski M, Kowalski ML. Endocrine disrupters – potential modulators of the immune system and allergic response. *Allergy* 2006;61(11):1326–35. https://doi.org/10.1111/j.1398-9995.2006.01135.x

[11] Samsel A, Seneff S. Glyphosate's Suppression of Cytochrome P450 Enzymes and Amino Acid Biosynthesis by the Gut Microbiome: Pathways to Modern Diseases. *Entropy* 2013;15(4):1416–63. https://doi.org/10.3390/e15041416

[12] Je B, Seneff S. The Possible Link between Autism and Glyphosate Acting as Glycine Mimetic - A Review of Evidence from the Literature with Analysis. *J Mol Genet Med* 2015;09(04). https://doi.org/10.4172/1747-0862.1000187

[13] Seneff S, Swanson N, Li C. Aluminum and Glyphosate Can Synergistically Induce Pineal Gland Pathology: Connection to Gut Dysbiosis and Neurological Disease. *Agric Sci* 2015;06(01):42–70. https://doi.org/10.4236/as.2015.61005

[14] Rull RP, Ritz B, Shaw GM. Neural Tube Defects and Maternal Residential Proximity to Agricultural Pesticide Applications. *Am J Epidemiol* 2006;163(8):743–53. https://doi.org/10.1093/aje/kwj101

[15] Paganelli A, Gnazzo V, Acosta H, López SL, Carrasco AE. Glyphosate-Based Herbicides Produce Teratogenic Effects on Vertebrates by Impairing Retinoic Acid Signaling. *Chem Res Toxicol* 2010;23(10):1586–95. https://doi.org/10.1021/tx1001749

[16] Cattani D, De Liz Oliveira Cavalli VL, Heinz Rieg CE, Domingues JT, Dal-Cim T, Tasca CI, Mena Barreto Silva FR, Zamoner A. Mechanisms underlying the neurotoxicity induced by glyphosate-based herbicide in immature rat hippocampus: Involvement of glutamate excitotoxicity. *Toxicology* 2014;320:34–45. https://doi.org/10.1016/j.tox.2014.03.001

[17] Thongprakaisang S, Thiantanawat A, Rangkadilok N, Suriyo T, Satayavivad J. Glyphosate induces human breast cancer cells growth via estrogen receptors. *Food Chem Toxicol* 2013;59:129–36. https://doi.org/10.1016/j.fct.2013.05.057

[18] Samsel A, Seneff S. Glyphosate, pathways to modern diseases II: Celiac sprue and gluten intolerance. *Interdiscip Toxicol* 2013;6(4):159–84. https://doi.org/10.2478/intox-2013-0026

[19] Jayasumana C, Gunatilake S, Senanayake P. Glyphosate, hard water and nephrotoxic metals: are they the culprits behind the epidemic of chronic kidney disease of unknown etiology in Sri Lanka? *Int J Environ Res Public Health* 2014;11(2):2125–47. https://doi.org/10.3390/ijerph110202125

[20] Jayasumana C, Gunatilake S, Siribaddana S. Simultaneous exposure to multiple heavy metals and glyphosate may contribute to Sri Lankan agricultural nephropathy. *BMC Nephrol* 2015;16(1):103. https://doi.org/10.1186/s12882-015-0109-2

[21] Bafei EP, Metowogo K, Eklu-Gadegbeku K. Study of the Health Impact of Glyphosate Misuse in Two Prefectures in Togo and Evaluation of Its Bioaccumulation in Yam. *Occup Dis Environ Med* 2021;09(04):199–213. https://doi.org/10.4236/odem.2021.94015

[22] Costas-Ferreira C, Durán R, Faro LRF. Toxic Effects of Glyphosate on the Nervous System: A Systematic Review. *Int J Mol Sci* 2022;23(9):4605. https://doi.org/10.3390/ijms23094605

[23] Klátyik S, Simon G, Oláh M, Takács E, Mesnage R, Antoniou MN, Zaller JG, Székács A. Aquatic ecotoxicity of glyphosate, its formulations, and co-formulants: evidence from 2010 to 2023. *Environ Sci Eur* 2024;36(1):22. https://doi.org/10.1186/s12302-024-00849-1

[24] Bradley PM, Journey CA, Romanok KM, Barber LB, Buxton HT, Foreman WT, Furlong ET, Glassmeyer ST, Hladik ML, Iwanowicz LR, Jones DK, Kolpin DW, Kuivila KM, Loftin KA, Mills MA, Meyer MT, Orlando JL, Reilly TJ, Smalling KL, Villeneuve DL. Expanded Target-Chemical Analysis Reveals Extensive Mixed-Organic-Contaminant Exposure in U.S. Streams. *Environ Sci Technol* 2017;51(9):4792–802. https://doi.org/10.1021/acs.est.7b00012

[25] Calvet R. Les pesticides dans le sol: conséquences agronomiques et environnementales. France agricole éditions; 2005

[26] Marc J. Effets toxiques d'herbicides à base de glyphosate sur la régulation du cycle cellulaire et le développement précoce en utilisant l'embryon d'oursin. PhD Thesis. Rennes 1, 2004

[27] LABAD R. Effets environnementaux du désherbage chimique associé au semis direct. PhD Thesis. 2018

[28] BOUIDIA C, MAKKEB A. Etude de l'effet de l'application de glyphosate et sa biodégradation par la densité bactérienne d'un sol oasien; cas du sol de l'exploitation de l'université de Ouargla. PhD Thesis. UNIVERSITE KASDI MERBAH OUARGLA, n.d.

[29] Wang M, Zhang G, Qiu G, Cai D, Wu Z. Degradation of herbicide (glyphosate) using sunlight-sensitive MnO 2 /C catalyst immediately fabricated by high energy electron beam. *Chem Eng J* 2016;306:693–703. https://doi.org/10.1016/j.cej.2016.07.063

[30] Rajasulochana P, Preethy V. Comparison on efficiency of various techniques in treatment of waste and sewage water – A comprehensive review. *Resour-Effic Technol* 2016;2(4):175–84. https://doi.org/10.1016/j.reffit.2016.09.004

[31] Mansour HB, Boughzala O, Dridi dorra, Barillier D, Chekir-Ghedira L, Mosrati R. Les colorants textiles sources de contamination de l'eau: CRIBLAGE de la toxicité et des méthodes de traitement. *Rev Sci L'eau* 2011;24(3):209–38

[32] Hartemann P. Contamination des eaux en milieu professionnel. *EMC-Toxicol-Pathol* 2004;1(2):63–78

[33] Bamba D, Dongui B, Trokourey A, Zoro GE, Athéba GP, Robert D, Wéber JV. Etudes comparées des méthodes de préparation du charbon actif, suivies d'un test de dépollution d'une eau contaminée au diuron. *J Soc Ouest-Afr Chim* 2009;28:41–52

[34] Sen K, Chattoraj S. A comprehensive review of glyphosate adsorption with factors influencing mechanism: Kinetics, isotherms, thermodynamics study. Intell. Environ. Data Monit. Pollut. Manag. Elsevier; 2021;93–125. https://doi.org/10.1016/B978-0-12-819671-7.00005-1

[35] Grant GA, Fisher PR, Barrett JE, Wilson PC. Removal of Agrichemicals from Water Using Granular Activated Carbon Filtration. *Water Air Soil Pollut* 2019;230(1):7. https://doi.org/10.1007/s11270-018-4056-y

[36] Rio S, Le Coq L, Faur C, Lecomte D, Le Cloirec P. Preparation of Adsorbents from Sewage Sludge by Steam Activation for Industrial Emission Treatment. *Process Saf Environ Prot* 2006;84(4):258–64. https://doi.org/10.1205/psep.05161

[37] Le charbon actif, l'or noir du Japon. *CURE Nat* n.d. http://www.curenature.fr/1/post/2021/09/pourquoi-utiliser-du-charbon-actif.html (accessed April 6, 2024)

[38] El Qada EN, Allen SJ, Walker GM. Influence of preparation conditions on the characteristics of activated carbons produced in laboratory and pilot scale systems. *Chem Eng J* 2008;142(1):1–13

[39] Wang S, Seiwert B, Kästner M, Miltner A, Schäffer A, Reemtsma T, Yang Q, Nowak KM. (Bio)degradation of glyphosate in water-sediment microcosms – A stable isotope

co-labeling approach. *Water Res* 2016;99:91–100. https://doi.org/10.1016/j.watres.2016.04.041

[40] Barathi M, Santhana Krishna Kumar A, Rajesh N. Efficacy of novel Al–Zr impregnated cellulose adsorbent prepared using microwave irradiation for the facile defluoridation of water. *J Environ Chem Eng* 2013;1(4):1325–35. https://doi.org/10.1016/j.jece.2013.09.026

[41] Gimsing AL, Szilas C, Borggaard OK. Sorption of glyphosate and phosphate by variable-charge tropical soils from Tanzania. *Geoderma* 2007;138(1–2):127–32. https://doi.org/10.1016/j.geoderma.2006.11.001

[42] Jiang X, Ouyang Z, Zhang Z, Yang C, Li X, Dang Z, Wu P. Mechanism of glyphosate removal by biochar supported nano-zero-valent iron in aqueous solutions. *Colloids Surf Physicochem Eng Asp* 2018;547:64–72. https://doi.org/10.1016/j.colsurfa.2018.03.041

[43] Khoury GA, Gehris TC, Tribe L, Torres Sánchez RM, Dos Santos Afonso M. Glyphosate adsorption on montmorillonite: An experimental and theoretical study of surface complexes. *Appl Clay Sci* 2010;50(2):167–75. https://doi.org/10.1016/j.clay.2010.07.018

[44] Damonte M, Torressanchez R, Dossantosafonso M. Some aspects of the glyphosate adsorption on montmorillonite and its calcined form. *Appl Clay Sci* 2007;36(1–3):86–94. https://doi.org/10.1016/j.clay.2006.04.015

[45] Ren Z, Dong Y, Liu Y. Enhanced Glyphosate Removal by Montmorillonite in the Presence of Fe(III). *Ind Eng Chem Res* 2014;53(37):14485–92. https://doi.org/10.1021/ie502773j

[46] Guo F, Li D, Fein JB, Xu J, Wang Y, Huang Q, Rong X. Roles of hydrogen bond and ion bridge in adsorption of two bisphenols onto montmorillonite: an experimental and DFT study. *Appl Clay Sci* 2022;217:106406. https://doi.org/10.1016/j.clay.2022.106406

[47] Yang S, Zhang B, Zheng X, Chen G, Ju Y, Chen B-Z. Insight into the adsorption mechanisms of CH4, CO2, and H2O molecules on illite (001) surfaces: A first-principles study. *Surf Interfaces* 2021;23:101039. https://doi.org/10.1016/j.surfin.2021.101039

[48] Laibi AB, Gomina M, Sorgho B, Sagbo E, Blanchart P, Boutouil M, Sohounhloule DKC. Caractérisation physico-chimique et géotechnique de deux sites argileux du Bénin en vue de leur valorisation dans l'éco-construction. *Int J Biol Chem Sci* 2017;11(1):499. https://doi.org/10.4314/ijbcs.v11i1.40

[49] Hamza A, Hussein IA, Mahmoud M. Introduction to reservoir fluids and rock properties. Dev. Pet. Sci., vol. 78. Elsevier; 2023;1–19. https://doi.org/10.1016/B978-0-323-99285-5.00003-X

[50] Ruiz-García M, Villalobos M, Antelo J, Martínez-Villegas N. Tl(I) adsorption behavior on K-illite and on humic acids. *Appl Geochem* 2022;138:105220. https://doi.org/10.1016/j.apgeochem.2022.105220

[51] Kresse G, Joubert D. From ultrasoft pseudopotentials to the projector augmented-wave method. *Phys Rev B* 1999;59(3):1758–75. https://doi.org/10.1103/PhysRevB.59.1758

[52] Perdew, J.P., Burke, K., and Ernzerhof, M. Generalized gradient approximation made simple. *Phys Rev Lett* 1996;77:3865-3868.

[53] Grimme S. Semiempirical GGA-type density functional constructed with a long-range dispersion correction. *J Comput Chem* 2006;27(15):1787–99. https://doi.org/10.1002/jcc.20495

[54] Haus JW. Nanophotonic devices. Fundam. Appl. Nanophotonics. Elsevier; 2016;341–95. https://doi.org/10.1016/B978-1-78242-464-2.00011-7

[55] Grimme S. Accurate description of van der Waals complexes by density functional theory including empirical corrections. *J Comput Chem* 2004;25(12):1463–73. https://doi.org/10.1002/jcc.20078

[56] Daouli A, Hessou EP, Monnier H, Dziurla M-A, Hasnaoui A, Maurin G, Badawi M. Adsorption of NO, NO_2 and H_2O in divalent cation faujasite type zeolites: a density functional theory screening approach. *Phys Chem Chem Phys* 2022;24(25):15565–78. https://doi.org/10.1039/D2CP00553K

[57] Jabraoui H, Hessou EP, Chibani S, Cantrel L, Lebègue S, Badawi M. Adsorption of volatile organic and iodine compounds over silver-exchanged mordenites: A comparative periodic DFT study for several silver loadings. *Appl Surf Sci* 2019;485:56–63. https://doi.org/10.1016/j.apsusc.2019.03.282

[58] Momma K, Izumi F. *VESTA* : a three-dimensional visualization system for electronic and structural analysis. *J Appl Crystallogr* 2008;41(3):653–8. https://doi.org/10.1107/S0021889808012016

[59] Wang V, Xu N, Liu J-C, Tang G, Geng W-T. VASPKIT: A user-friendly interface facilitating high-throughput computing and analysis using VASP code. *Comput Phys Commun* 2021;267:108033. https://doi.org/10.1016/j.cpc.2021.108033

[60] Wang M, Rivenbark KJ, Phillips TD. Adsorption and detoxification of glyphosate and aminomethylphosphonic acid by montmorillonite clays. *Environ Sci Pollut Res* 2022;30(5):11417–30. https://doi.org/10.1007/s11356-022-22927-8